Energy and Buildings 128 (2016) 56–67

Contents lists available at ScienceDirect

Energy and Buildings

journal homepage: www.elsevier.com/locate/enbuild

The effect of time-of-use tariffs on the demand response flexibility of an all-electric smart-grid-ready dwelling

Fabiano Pallonetto[a,*], Simeon Oxizidis[b], Federico Milano[c], Donal Finn[d]

[a] Electricity Research Centre, University College Dublin, Dublin, Ireland
[b] International Energy Research Centre, Tyndall National Institute, Cork, Ireland
[c] School of Electrical & Electronic Engineering, University College Dublin, Dublin, Ireland
[d] School of Mechanical and Materials Engineering, University College Dublin, Ireland

ARTICLE INFO

Article history:
Received 28 October 2015
Received in revised form 23 May 2016
Accepted 13 June 2016
Available online 21 June 2016

Keywords:
Residential building
Control algorithms
Demand response
Renewable energy
Time of use tariff
Energy management system
Thermal storage
Building simulation
Flexibility
Smart grid

ABSTRACT

The paper is concerned with the development and evaluation of control algorithms for the implementation of demand response strategies in a smart-grid enabled all-electric residential building. The dwelling is equipped with a 12 kW heat pump, a 0.8 m^3 water storage tank, a 6 kW photovoltaic (PV) array, solar thermal collectors for domestic hot water heating and an electric vehicle. The building, located in Ireland, is fully instrumented. An EnergyPlus building simulation model of the dwelling was developed and calibrated using monitored data from the building. The developed model is used to assess the effectiveness of demand response strategies using different time-of-use electricity tariffs in conjunction with zone thermal control. A reduction in generation cost (−22.5%), electricity end-use expenditure (−4.9%) and carbon emission (−7.6%), were estimated when DR measures were implemented and compared with a baseline system. Furthermore, when the zone control features were enabled, the efficiency of the control improved significantly giving, an overall annual economic saving of 16.5% for the residential energy cost. The analysis also identified an annual reduction of consumer electricity consumption of up to 15.9%, lower carbon emissions of 27% and facilitated greater utilisation of electricity generated by grid-scale renewable resources, resulting in a reduction of generation costs for the utility of up to 45.3%.

1. Introduction

Over the past decade, government policy initiatives have established ambitious targets for the increased penetration of renewable generation in power systems to combat the threat of climate change. Large-scale renewable generation penetration presents major challenges for Transmission System Operator (TSO), challenging established methods of balancing supply and demand [1]. Traditionally, supply-demand balancing measures have been achieved by controlling the output of conventional generation in response to changes in the demand. With increasing renewable generation, however, there are greater fluctuations on the supply side, requiring faster-balancing response from grid operators. Conventional generation units, however, may not have sufficient ramping capabilities to counter rapid fluctuations in renewable energy. In Ireland and UK, the domestic sector accounts for more than 27% of the total end-use electricity consumption [2]. This electricity demand peaks in winter due to increased lighting and heating demand, and these peaks result in high wholesale electricity prices and reduced reliability due to tight generation reserve margins. Without sufficient forward planning on the generation side, high penetration levels of renewable generation and high demand peaks may lead to system contingencies, or in an extreme case, system blackouts [3]. Demand Response (DR) is one of the Demand Side Management (DSM) measure that has being promoted since 1970s in the UK and other countries, so as to reduce high winter peaks as well as avoiding associated grid upgrade costs [4]. More recently, there has been renewed interest in DR as a mechanism to increase the percentage of renewable energies in the system [5]. Demand response (DR) has been defined as "changes in electricity use by demand-side resources from their normal consumption patterns in response to changes in the price of electricity or to incentive payments designed to induce lower electricity use at times of high wholesale market prices or when system reliability is jeopardized" [5]. DR can be price-based such as Real Time Price (RTP), Critical Peak Price (CPP) and Time of Use Tariff (TOU) or incentive-based, where the participating customers are rewarded

* Corresponding author. Room 338, Eng. Building, Electricity Research Centre, University College Dublin, Belfield, Dublin 4, Ireland.
E-mail address: fabiano.pallonetto@ucdconnect.ie (F. Pallonetto).

http://dx.doi.org/10.1016/j.enbuild.2016.06.041
0378-7788/

Nomenclature

C_e	electricity price (€\kWh)
C_{set}	circulation pump status
COP_{hp}	heat pump average COP
Cpw	specific heat capacity J\(kg K)
F	forcing flexibility
M	TES water mass
P_{hp}	heat pump energy consumption (kWh)
PV	PV electricity production
S	shifting flexibility
T_{bd}	TES setpoint bandwidth (°C)
T_{in}	internal zone temperature (°C)
$T_{\max}$	TES maximum set point temperature (°C)
$T_{\min}$	TES minimum set point temperature (°C)
T_{out}	outside temperature (°C)
T_{set}	TES minimum set point temperature (°C)
T_{set}	temperature set point (°C)
T_{tk}	TES temperature (°C)

for reducing their load when requested by an aggregator or TSO [4]. DR measures can have different levels of automation. Manual DR requires human intervention to shift or force loads or to change set point temperature. In the semi-automated measures, an energy manager operates a centralised system to initialise the demand response strategy. In the fully automated DR strategies, an external communication signal triggers the pre-programmed methods, and thus does not require human interaction. In the latter case, the responsible subject should be able to override the event at any time [6]. Among several challenges for DR schemes, is the reliable availability of the resources. The DR system may not be in a position to respond to high peak prices. Capturing the time-varying availability using advanced metering and tailored metrics is a necessity for the success of DR schemes. Furthermore, the impact of stochastic consumer behaviour can affect the benefit of DR programs. However, such irregularities can be smoothed by resource aggregation. As noted in Nolan et al. [7], the aggregation of few thousands of households represents a stable DR system resource. Hence, the domestic sector electricity demand can provide services such as spinning reserve, frequency control or short term operating reserve.

Therefore, exploiting residential flexible electricity demand, facilitated by clear and appropriate regulation to promote the operation of demand response programmes, can be part of the solution for the power system balancing challenges [8]. In this work, demand flexibility is considered as the ability to force (activate) or shift (defer) building electrical energy consumption, based on supply constraints at a current or future time. In a residential building, the flexible loads can be appliances, electric vehicles or space and water heating systems. Flexibility is generally enabled by means of energy storage systems, which can be electrical (e.g., electrical vehicle, battery) or active thermal storage (e.g., phase change material, water tank) or passive thermal storage (e.g., building fabric). By using an Energy Management System (EMS), capable of integrated control of the overall domestic electrical demand, it is possible to dynamically adapt the supply to demand response signals, thereby providing short-term reserve to the power system without affecting the thermal comfort of the occupants. In fact, with the improvements in computer and communication technology, it is possible to conceive a fully automated DR systems in the domestic sector. However, to utilize residential buildings as flexible electricity demand resource, additional communication infrastructure and large-scale data is required. The data required includes real-time prices, weather forecasts, energy mix generation and end-use consumption. To this end, the upcoming smart grid has the objective to provide a bidirectional communication system to exchange data from electricity generation to end-use though better control. Such technologies aim to increase the resiliency of the network, integrate a higher percentage of renewable energy and storage resources, as well as maximising asset utilization. Alam et al. [9] define a smart dwelling as the end node of the smart grid which provides services in the form of ambient intelligence, remote home control, or home automation. In a smart house, the EMS adapts the house energy consumption to the overall grid requirements without affecting the comfort of the occupants. Furthermore, each dwelling or node of the smart grid has the possibility to broadcast information about its electricity consumption profile and status. Advanced communication infrastructure, along with appropriate end-use optimization algorithms, can potentially allow end-users to shape their electricity consumption according to price signals, which would follow the real-time balance between renewable energy generation and power system demand. The use of price signals based on TOU tariffs to manage household electricity demand has been extensively explored in the literature [4]. Nevertheless exposing end-users to price variations does not necessarily lead to energy cost savings [10]. Especially for residential buildings, the daily economic benefit of peak reduction may be of little financial incentive to the consumer, and thus may not result in a change in consumer behaviour. For this reason, the majority of the projects in the DR area include the use of information technology to develop automated systems for the management of the end-use participation [11]. A residential building energy management system can analyse the data provided by the Smart Grid to trigger DR measures to assist grid operators in maintaining the supply-demand balance on the power system. At the same time, the system tries to optimise electricity consumption and production in a manner that delivers the households energy services demands while minimising their energy costs. Furthermore, increasing the integration of advanced energy management systems presupposes significant electrification of building thermal loads, on-site generation and highly energy efficient building envelopes.

In the future, electrification of domestic heating systems through the deployment of heat pumps is expected to alter residential electrical energy demand patterns substantially [12]. Hydronic heat pumps are an especially efficient way of electrifying residential thermal loads and can be easily coupled with thermal energy storage systems, either active, such as water tanks, or passive, such as building thermal mass. This trend towards greater levels of electrification of thermal loads in buildings is already present with IEA [13] anticipating significant growth in the number of heat pump installations worldwide in the coming decade. As illustrated by Hong et al. [14], heat pumps can provide flexibility while meeting the end-user thermal comfort expectations. A simulation desk study performed as part of this research illustrates how the comfort temperature settings can affect the available shifting time provided by the combination of a heat pump and thermal storage. In energy efficient buildings, electrically driven heating systems such as heat pumps in conjunction with sophisticated control algorithms can provide demand response capabilities to the power grid [15]. However, according to Fuller et al. [16], until equipment and algorithms can be validated and benchmarked, it is difficult for utilities and regulators to install, operate and exploit these new resources. Therefore, the use of advanced analytical tools, building simulation software and appropriate metrics can help to assess the value and the risks of new technologies that provide electricity demand flexibility.

In the literature, there are numerous examples on how to exploit building flexibility and quantify its value at an aggregated level. Nuytten et al. [17] assessed the thermal flexibility of a centralised heating system and a thermal storage facility of 800 kWh connected

to an aggregate residential district of 100 buildings. Such analysis is useful for small district heating, but it is challenging to apply this analysis to a single building where occupancy profiles and different heating systems could affect the results significantly. Furthermore, Mohsenian-Rad et al. described an optimal residential control algorithm capable of reducing the peak energy load and shift loads to periods of lower electricity prices [18]. The assessment is based on a mathematical model which cannot be easily implemented in a real building. Other researchers have focused on the EMS hardware design incorporating demand response capabilities [19] or on how to reduce the electricity cost for a single residential building [20]. Kolokotsa et al. [21] developed an integrated indoor management system for buildings using a fuzzy controller. They were able to consider the comfort constraints of the occupants by tuning and optimising the system using two demonstration buildings in Greece. However, the control algorithm assessment in real buildings could require years of analysis before having consistent results, and it is difficult to validate the benefit of small control flow variations.

Tahersima et al. [15] highlighted how a ground source residential heat pump controlled by a smart algorithm can compensate for grid imbalances utilising the thermal storage of the building mass within a thermal comfort band. In order to maximise the stored energy while keeping the temperature within an established range, a flexible temperature set-point was defined, which was adjusted according to electricity tariffs. It was clear from this research that the thermal mass associated with the residential building can reduce undesirable temperature fluctuations and maintain occupant thermal comfort. Nevertheless, further assessment of the overall economic and environmental benefits of these solutions are required.

The contribution of this paper is the development of a demand response control algorithm that reduces the overall cost of energy and annual carbon emissions for different stakeholders. The objective of the control algorithm is to minimise energy costs for both the house owner and electricity generation, by taking advantage of time-of-use electricity tariffs, as well as enabling reductions in CO_2 emissions. The algorithms use thermal comfort criteria as a constraint and facilitates a clear assessment of benefits derived, based on market and power grid data. A key feature of the implemented control system is a dynamic assessment of the system flexibility which is capable of being calculated every 15 min, and thus can be used by DR aggregators to activate demand response actions in real time. To assess the benefit of the control system, a software model of an all-electric dwelling and its associated energy conversion system was developed using EnergyPlus and calibrated using on-site data, which was monitored over a full heating season. The paper is organised as follows: Section 2 includes the description of the building, the installed energy systems, the occupancy profile and the tariffs used. Section 3 describes the control algorithm. In Section 4, the performance results are presented utilising different demand response strategies. Section 5 concludes the paper.

Fig. 1. Test bed house and EnergyPlus model.

2. Building description

The all-electric building used as a test bed in the current work is situated in a rural location in eastern Ireland (Fig. 1). The dwelling was retrofitted in 2012 and fully instrumented. The building was renovated to meet 2020 scenario as outlined in the Residential Energy Roadmap for Ireland [22]. This publication sets out scenarios that show what reduction level of CO_2 emissions is achievable with different retrofit measures. The scenarios include a higher penetration of solar thermal and solar PV, storage heating and heat pump systems. The majority of these systems are present in the test building considered in the current study. Moreover, the test building energy consumption and the CO_2 emissions are also aligned with the 2020 scenario. Furthermore, the building was equipped with technologies that have been identified by the Irish Commission for Energy Regulation as appropriate to offer demand response services. These technologies, which if adopted in the residential sector would enable demand response in the Irish power system [23], are summarised in Table 1, where their presence in the test bed building is also reported. One measure absent from the current building is frequency response capabilities, which would typically be enabled by home automation systems. Given the rural position of the building and the associated network distribution system layout, the dwelling is at the terminal side of a distribution branch. In this location, the electricity supply is more prone to voltage fluctuations that mitigate against the implementation of frequency response measures. An EnergyPlus building model was developed and calibrated against metered data using an hourly resolution according to ASHRAE recommendations [24]. The Average Percentage Error (APE) was used to indicate the accuracy of the calibrated building

Table 1
CER Index: demand response measures [23].

Technologies	Delivery cost	Ranking	Test bed house
Energy efficiency – domestic	Medium	High	Present
Smart meter system – dynamic ToU tariff	Medium	High	
Home automation – direct load control	Medium	High	Present
Home automation – autonomous	Low	High	Present
Home automation – frequency-responsive	Medium	High	
Storage – heat	Low	High	Present
Smart meter system – advanced displays	Low	Medium	Present
Smart meter system – static ToU tariff	Low	Medium	Present
Electric vehicles – price responsive charging	Medium	Medium	
Behavioural change – education	Low	Low	Present
Heat pumps – fitted with storage	High	Low	Present
Storage – electric	High	Low	
Electric vehicles – night charge	Low	Neutral	Present
Electric vehicles – hybrid vehicles	Medium	Neutral	
Microgeneration – controllable	Low	Neutral	Present

Table 2
U-value of different building elements.

Building element	*U*-value test building (W/m²K)	*U*-value Irish building regulations [25] (W/m²K)
Walls	0.25	0.21
Roof	0.25	0.21
Windows	1.7	1.6
Floor	0.21	0.21

model and is based on an annual error specification calculated using one year of data (2012).

2.1. Architecture and building physics

The dwelling, a single storey building, was constructed using a two leaf concrete wall with core insulation. Therefore, the inner wall displays significant passive thermal energy storage capacity. The floor area is 205 m^2 and the overall window to wall ratio is 15%, with a 22% and 10% ratio on the south and north facades, respectively. The house has 12 rooms and an unused attic space at roof level. Although its architectural characteristics are those of a typical rural Irish bungalow dwelling of the 1970s, its fabric specifications are very close to the current Irish building regulation values [25] as outlined in Table 2. According to [26], the building category considered in the current work is classified as a detached house, which represents 40% of the Irish building stock and is the most common single building category.

2.2. HVAC and energy systems

For space heating, the house is equipped with a 12 kW ground source heat pump, which is connected to a hot water tank of 0.8 m^3 for thermal storage, and an associated hydronic heating system. Convectors are present in each room, while there is an additional 5 kW wood stove in the kitchen. The wood stove is used only during the heating period, from October to April. A photovoltaic panel array consisting of 30 panels, of a total nominal power of 6 kWp is also installed. It is located 30 m from the house and any power losses from cables are taken into account. The PV system was metered for one year with a 15 min resolution. The electricity produced by the PV system and the EnergyPlus model was found to be accurate to within APE ±5.8%. Solar thermal collectors of surface area 6.15 m^2 are used for heating of Domestic Hot Water (DHW) in conjunction with a 250 l water storage tank. A 2 kW electric immersion heater is used as backup. The water tank is modelled in EnergyPlus as a fully mixed system [27]. The overall DHW system was calibrated with measured data and was found to be accurate to within APE ±13%.

2.3. Air exchange

The building is equipped with a Heat recovery ventilation (HRV) system with air extraction points located in the kitchen and bathroom. The particular HRV system has an average sensible heat transfer effectiveness of 80% and operates only during the heating period while during summer, natural ventilation (window opening) is being used. Based on the approach outlined in [28], the combined infiltration and ventilation rates were adjusted such that an average annual value was utilised. For infiltration and ventilation purposes, the building is divided into two sections with the following ACH settings: a kitchen/living/bathroom zone (ACH 1.5) and a sleeping/utility zone (ACH 1.0). Infiltration and ventilation rates are adjusted in each time-step using weather data (wind speed and temperature differential between indoors and outdoors) according to ASHRAE [29]. Therefore, seasonal (summer/winter) and daily (day/night) variations of both infiltration and ventilation rates were taken into account based on environmental conditions resulting in modifications to the above design flow rates.

2.4. Electric car

A Nissan Leaf with a 24 kWh battery pack is used for daily commuting of approximately 50 km. According to Smith [30], the energy consumption by Electric Car (EV) depends on the season due to the air conditioning requirements of the cabin, which can significantly affect the energy performance of the car. The electricity consumption of the EV for the system simulation model was set to 150 Wh/km during the summer and 250 Wh/km during the winter. The car is charged overnight when electricity prices are lower. The daily energy requirement of the car is 12.5 kWh in the winter and 7.5 kWh in the summer. During night time charging, the electricity drawn is assumed to follow the pattern suggested by Marra et al. [31]. The model used in EnergyPlus was found to be accurate to within APE ±3.5% of the referenced data.

2.5. Occupancy profiles

Two adults occupy the house. Occupancy profiles, domestic hot water usage patterns, use of electric equipment and lighting, and the respective distribution of internal heat gains were calculated based on the national time of survey resident activity data. As outlined in [32], using time of use data, Markov Chain Monte Carlo techniques were applied to develop high time resolution and disaggregated residential appliance electricity use patterns. In the current work, daily power consumption patterns, for different household sizes and different day types, were quantitatively and qualitatively validated against metered data. The synthesized profiles were calibrated with the appropriate occupant adjustments to replicate better the real life activity patterns.

2.6. Weather data

The weather data used was collected from the closest available weather station (Dublin Airport) which is located 35 km from the dwelling. In order to generate an appropriate weather data file, measured data from 2012 was analyzed using the Real Time Weather Converter software package [33]. This tool creates weather files by combining observed weather data from the Integrated Surface Database (ISD) with the STRÅNG mesoscale solar radiation model.

2.7. Building model

The building model was calibrated with measured data from the site. A 15 min time step was used for the simulations. Given that the objective of the paper is to assess the building demand flexibility as secondary reserve and not for frequency response, a 15 min resolution was considered to be sufficient according to the technical specifications associated with the provision of ancillary services in the Irish electricity market [34].

2.8. Electricity price

During the last decade, time of use electricity tariffs are increasingly being utilised in the US and to a lesser extent in European markets [23]. In 2010, the Irish Commission for Energy Regulation initiated a residential smart meter trial, with associated tariffs (A, B, C, D, Flatrate) as shown in Table 3 [35]. The pricing scheme reflects the trend of the Irish System Marginal Price (SMP) Average and consequently of the overall electricity demand. These tariffs, along

Table 3
Time of use electricity tariffs (€/kWh).

	Weekdays						Weekdays					
	A	B	C	D	Flat	SMP (avg)	A	B	C	D	Flat	SMP (avg)
00:00–08:00	0.12	0.11	0.1	0.09	0.135	0.046	0.12	0.11	0.1	0.09	0.135	0.044
08:00–17:00	0.14	0.135	0.13	0.125	0.135	0.065	0.14	0.135	0.13	0.125	0.135	0.062
17:00–19:00	0.2	0.26	0.32	0.38	0.135	0.097	0.14	0.135	0.13	0.125	0.135	0.088
19:00–23:00	0.14	0.135	0.13	0.125	0.135	0.071	0.14	0.135	0.13	0.125	0.135	0.067
23:00–00:00	0.12	0.11	0.1	0.09	0.135	0.053	0.12	0.11	0.1	0.09	0.135	0.053

Table 4
Control system for each case.

Parameter	Description	Baseline	Case 1	Case 2	Case 3
Building setpoints	No. of programmable thermostats	1	1	5	5
Thermal storage	Min temperature	40 °C	40 °C	40 °C	35 °C
	Max temperature	55 °C	55 °C	55 °C	55 °C
PV system	Min HP activation power PV	Not applicable	3 kW	3 kW	2 kW
TES charging	Charging start time before peak	Not applicable	2 h	2 h	2 h

with a PV electricity export of 0.09€ per kWh were used in the current work.

3. Demand response control algorithms

The demand response algorithm implemented in the current paper had to be capable of being integrated into a high-resolution simulation environment such as EnergyPlus while keeping any hardware installation as simple as practicable. This required the use of the simplified programming language embedded with the simulation engine (ERL) [27]. Due to the technical limits of the programming language, the selection of suitable controlling algorithms was limited. Other constraints include that the algorithm had to be adaptable to occupant comfort profiles without the need for processing historical data. Furthermore, residents should be able to override the algorithm on demand. A rule-based algorithm capable of been easily tuned by occupants based on their profile was therefore chosen, as it could be tested in the simulation environment while meeting all the mentioned requirements. The rule-based control algorithm was developed, tested and subjected to the three different case scenarios described in Table 4, as well as being compared with a baseline case. Control is based on a heuristic response to a time-of-use (TOU) price scheme described in Section 2.8. The control algorithm was embedded in an energy management system within the EnergyPlus model using the native programming language [36]. The objective function (Eq. (1)) of the energy management system is to reduce the owner energy cost while maintaining the comfort constraints (Eq. (2)), which can be written as follows:

$$\min_{(T_{tk}, C_{set})} \left(\sum_{t=1}^{24} C_e(t) P_e(t, T_{tk}, C_{set}) \right) \quad (1)$$

$$T_{set}(t) - T_{bd} \leq T_{\text{int}}(t) \leq T_{set}(t) + T_{bd} \quad t = 1, \ldots, 24 \quad (2)$$

$$T_{\min} \leq T_{tk} \leq T_{\max} \quad t = 1, \ldots, 24 \quad (3)$$

where $C_e(t)$ is the price of electricity (€/kWh) and P_e is the electricity consumption. $P_e(t, T_{tk}, C_{set})$ is the energy consumption in kWh of the building simulation model described in this research at each time step t. The cost optimisation depends on two control variables as follows: (i) the temperature of the tank (T_{tk}) which is maintained within the range $T_{\max}$ and $T_{\min}$ and, (ii) the energy supplied to the zones by means of the circulation pump which can be either ON or OFF (C_{set}). At each time step, the zone temperature (T_{int}) is maintained at set point as illustrate in Table 5 with an associated 2 °C bandwidth (i.e., ±1 °C around the setpoint), as shown in Eq. (2); while Eq. (3) constrains the storage tank temperature between its max and min temperature settings, as illustrated in Table 5. The algorithm, outlined in Fig. 2, has four input variables: the building zone temperature, the time, the PV electricity production rate and the storage tank temperature. These input variables are evaluated by the algorithm at each time step and control the heat pump and the circulation pump. The heat pump exchanges heat with the Thermal Energy Storage (TES) storage tank by means of a tank heat exchanger coil. The building hydronic circuit is coupled directly to the TES tank. The tank can also be by-passed, thereby allowing the dwelling to be heated directly. The control algorithm, as outlined in Fig. 2, utilises four input variables: time, building zone temperature, storage tank temperature and PV electricity production rate. The control algorithm optimises the charge of the TES and associated heating of the building, while the direct heating of the dwelling can only be manually enabled. The algorithm is based on four different rules as follows (see Fig. 2):

(Rule 1 Comfort constraint): This rule is activated whenever the building zone temperature is below the zone comfort constraint for the period, or when the photovoltaic electricity production is greater than the heat pump electrical demand. When this condition is verified, the heat pump is switched on to charge the TES system.

Table 5
Building thermostatic set points for each case.

Weekdays	Configuration 1 Baseline and Case 1		Configuration 2 Case 2 and Case 3		Weekends	Configuration 1 Baseline and Case 1	Configuration 2 Case 2 and Case 3
	Corridor	Bedrooms	Corridor	Bedrooms			
00:00–06:30	19 °C	19 °C	17 °C	17 °C	00:00–06:30		
06:30–09:00	18 °C	18 °C	19 °C	19 °C	06:30–09:00		
09:00–16:00	16 °C	16 °C	16 °C	16 °C	09:00–16:00	20 °C	20 °C
16:00–19:00	18 °C	18 °C	18 °C	16 °C	16:00–19:00		
19:00–24.00	18 °C	18 °C	18 °C	18 °C	19:00–23:59		

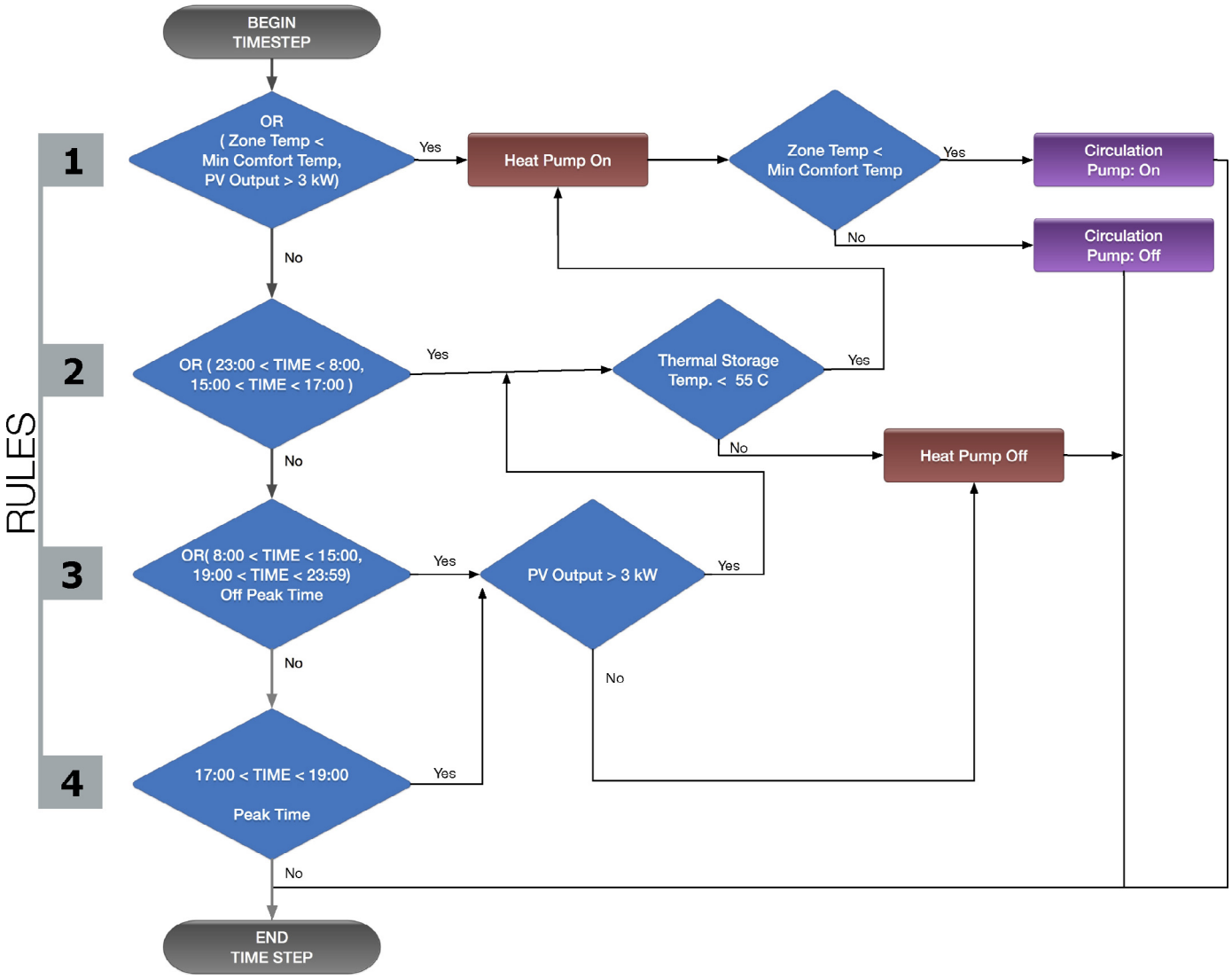

Fig. 2. Algorithm diagram flow chart.

If the inside temperature is below the comfort constraint, then the circulation pump is switched on to heat the building.

(Rule 2 TES charging time): This rule switches on the heat pump during the night (23:00–08:00) to charge the TES. When the TES is fully charged and the temperature is below the set point, then the circulation pump is switched on to supply heat to the house. During weekdays, between 15:00 and 17:00, the heat pump is switched on to charge the TES.

(Rule 3 Off-peak rule): During the off-peak period when the PV production is above the threshold, the heat pump is switched on to charge the TES. If the inside temperature is below the comfort constraint, then the circulation pump is also switched on to heat the building.

(Rule 4 On-peak rule): On the weekdays, the heat pump is switched off during the peak period (17:00–19:00) or when the house is not occupied (between 09:00–15:00), and the PV production is below the threshold illustrated in Table 4. The threshold corresponds to the heat pump nominal power consumption (3 kW). When the PV system produces electricity above this threshold, the heat pump is switched on to exploit PV electricity. The system is turned on for at least 1 h, using the weather data as forecast, in order to avoid intermittent switching of the heat pump.

3.1. Simulation parameters

An analysis of the simulation results using two configurations were chosen and these are illustrated in Table 4.

1. The first control parameter is based on the number of thermostatic controls in the house. For the Baseline Case and Case 1, a single temperature input variable, located in the hallway, controls the heating for the dwelling. For Cases 2 and 3, multiple temperature measurement control points are used.
2. The second control parameter is the minimum and maximum temperature set point of the thermal energy storage. For the Baseline Case and Case 1, the two set points are set at 40 °C and 55 °C. The maximum temperature of the TES is set with a 5 K difference between the outlet temperature from the heat pump (60 °C) and the TES set point. The minimum temperature was set at 40 °C. Case 3 uses 35 °C as the minimum temperature.
3. The third control parameter is the PV output. If the produced PV power is higher than the nominal maximum power demand of the heat pump (3 kW), the heat pump is switched on to charge the TES. Cases 1 and 2 use a threshold of 3 kW, while Case 3 lowers the threshold to 2 kW.

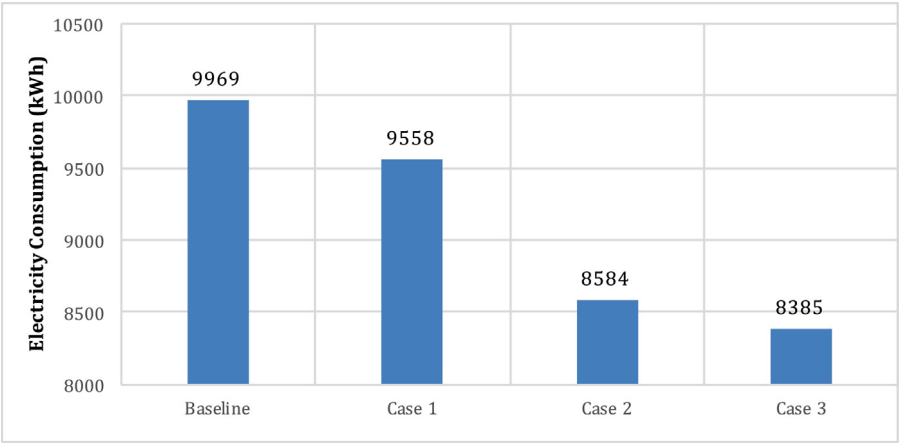

Fig. 3. Annual total electricity consumption.

Test simulations were performed and revealed that switching on the heating system 2 h before the peak electricity price was sufficient to store energy in the TES to maintain the comfort level while reducing the electricity consumption during the peak period.

3.2. Heating period and control

The heating season considered is between 01 January–30 April and 01 October–December 31 for the year 2012. The energy assessment uses two different thermostatic set point configurations utilised in four different cases. Each case represents a different rule setting of the algorithm where the objective is to reduce the overall electricity cost and increase the use of renewable energy or the energy stored in the tank. The baseline and Case 1 uses a single thermostatic set point (Configuration 1) for the whole building resulting in a partial cost reduction. The objective of Case 1 is to charge the storage tank fully and slightly increase the indoor temperature during the night, thereby slightly reducing the daily consumption. Meanwhile, Case 2 and 3 increase the energy efficiency of the system by using different set points for each room category (Configuration 2). In this specific test case, the set points of the kitchen and living room are ignored because the internal heat gains from the wood stove increase the ambient temperature beyond the set points without leading to a significant cost reduction. The two different thermostatic set point configurations are summarised in Table 5 and they represent the thermal comfort constraints. Given that the constraints above are satisfied for each case, the economic savings, the environmental impact, and the flexibility assessment of the strategies adopted are presented in Section 4.

4. Case study simulation results

Four metrics were used to assess the performance of the control algorithm and the energy flexibility in the building. The metrics are as follows:

- Consumer annual electricity consumption.
- Consumer annual electricity cost.
- Utility electricity cost.
- System flexibility potential.

Each of these metrics are considered in the following sections and are assessed against a baseline scenario.

4.1. Assessment of consumer annual electricity consumption

Fig. 3 illustrates the annual house electricity consumption which is imported from the grid for each case. Charging the storage tank before the peak period and subsequently utilising this energy during the peak period can result in additional energy consumption, due to additional temperature lift required to charge the TES system as well as the associated TES storage losses. Nevertheless, in the current work, the overall net electricity consumption has been reduced, due to the contribution of the PV system. This is because the heating system is switched on to charge the TES when the PV electricity generation reaches a threshold (Table 4). The net reduction attributed to the control strategy is equal to the power consumption difference between the Baseline and Case 1. However, in Case 2 and 3 compared to Baseline and Case 1, the net reduction is mainly due to the zone thermostatic set point strategy. Thus, during the unoccupied hours, the heating system operates, maintaining the temperature of the zones at the lower bound of the thermal comfort band, resulting in a lower electricity demand.

Fig. 4 shows the house electricity consumption minus the local renewable energy production for the baseline case and for each of the three cases. A 15 min time resolution is used, where each data point is determined by summing each time associated electricity consumption value (kWh) for that data point (365 instances) for the entire year. The PV contribution, is determined in a similar way, but is subtracted from the consumed electricity to allow a net value to be determined. The average SMP is also shown, which is based on the wholesale single island-wide price for each half hour trading period in a typical day [37]. For the baseline case, to meet the dwelling comfort constraints, the heat pump is switched on whenever needed, even during peak times. Case 1 exhibits increased electricity consumption between midnight and 0200 h due to a rebound effect associated with the earlier demand response action between 1800 and 1900 h. This results in additional electricity consumption in order to restore both the zone set point temperature (19 °C) and the tank set point temperature (55 °C) after the demand response event (see Tables 4 and 5). Cases 2 and 3, which exhibit broadly similar consumption patterns, result in a significant reduction of energy consumption during the peak period (17:00–19:00), compared to Case 1 and the baseline. For the period 21:00–23:00, additional electricity consumption is evident for Cases 2 and 3, compared to Case 1, due to the additional heating requirement to increase the bedroom temperatures from a set point of 16–18 °C after 1900 h (see Table 5). Moreover, Case 3 aims to increase the energy extraction from the TES, by using a lower temperature set point (35 °C) as specified in Table 5. Case 1 exhibits increased electricity consumption between midnight and 0200 h due to a rebound

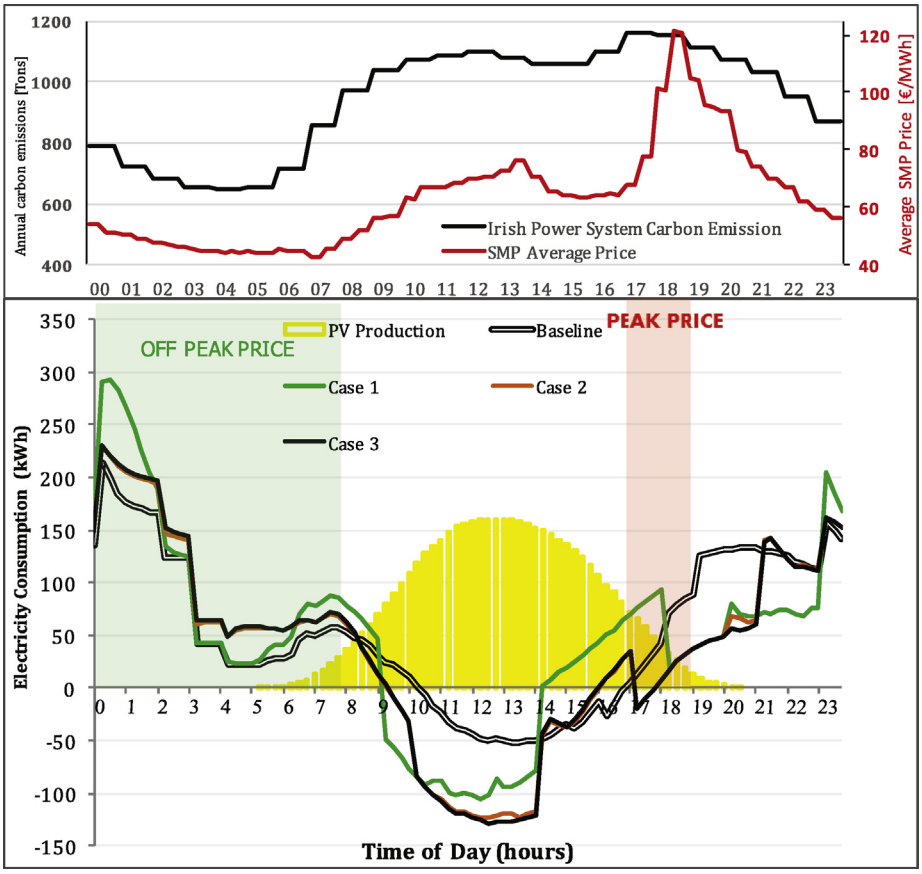

Fig. 4. Annual summated electricity consumption and power system CO_2 emission.

effect associated with the earlier demand response action between 1800 and 1900 h. This results in additional electricity consumption in order to restore both the zone set point temperature (19 °C) and the tank set point temperature (55 °C) after the demand response event (see Tables 4 and 5). Cases 2 and 3, which exhibit broadly similar consumption patterns, result in a significant reduction of energy consumption during the peak period (17:00–19:00), compared to Case 1 and the baseline. For the period 21:00–23:00, additional electricity consumption is evident for Cases 2 and 3, compared to Case 1, due to the additional heating requirement to increase the bedroom temperatures from a set point of 16–18 °C after 1900 h (see Table 5). Moreover, Case 3 aims to increase the energy extraction from the TES, by using a lower temperature set point (35 °C) as specified in Table 5.

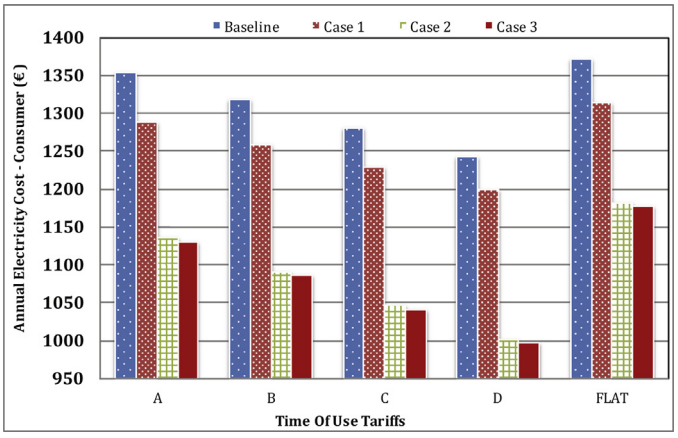

Fig. 5. Electricity cost for different time of use tariffs and algorithm cases.

4.2. Consumer electricity cost

Fig. 5 shows the annual electricity cost for the baseline and the three cases using the TOU tariffs outlined in Table 3. With reference to the baseline which exhibits the highest annual cost, Case 1 exhibits the next highest cost, which can be attributed to the use of a single thermostatic set point control for all controllable zones (bedrooms and corridor), resulting in additional heating of unoccupied zones. Considering Case 2, relative to the baseline, savings of between 15% for tariff A and 20% for tariff D (which most closely follows the SMP price) are evident. Case 3 is optimised to utilise PV electricity production, as well as using a lower TES set point (35 °C). Therefore, it exhibits the greatest savings relative to the baseline.

4.3. Utility electricity cost

Fig. 6 shows the generation cost using Irish electricity SMP prices [37]. The electricity consumption is multiplied by the

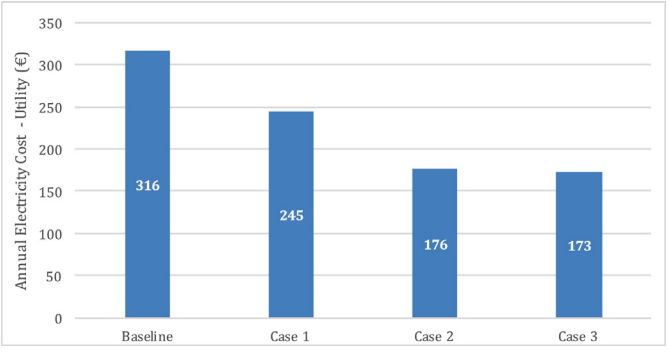

Fig. 6. Annual electricity generation costs.

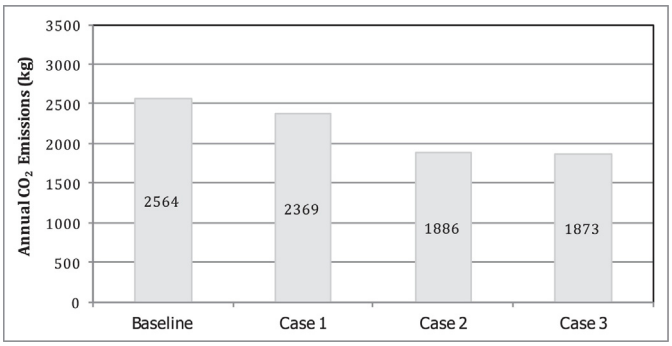

Fig. 7. Annual carbon dioxide emissions.

relevant SMP price for each time step in order to evaluate the yearly electricity production cost from a utility perspective. Considering Case 2, where the control strategy aims to move electricity consumption from peak (17:00–19:00) to off peak (15:00–17:00) times, a generation cost reduction from €316 to €245 is evident (22% reduction). Considering Case 3, a 45% (€173) reduction is evident. The difference between the SMP peak price and the off-peak can reach a ratio of 1–6. This ratio rationalizes such significant reduction of generation cost between the cases.

4.4. Environmental impact

Eirgrid, the Irish transmission system operator, provides 30 min averaged carbon emissions (g CO_2/kWh), based on technical data from all generation units, including renewable energy, for the overall production of electricity [38]. For 2012, the footprint varied from 29 (g CO_2/kWh) to 846 (g CO_2/kWh). Fig. 4 illustrates the annual carbon emissions per hour. The maximum annual carbon emission is verified during the peak time hours (1700–1900 h). Therefore, a significant reduction in CO_2 emission is expected as a result of the control algorithm. Fig. 7 illustrates the annual CO_2 footprint as determined for the baseline and the three cases. Case 3 is observed to give the greatest reduction, which is 74% relative to the baseline case, as PV power is used to charge the TES via the heat pump system whenever possible, thereby reducing the overall electricity drawn from the grid and consequently the associated carbon emissions.

4.5. System flexibility

In the current paper, system flexibility is defined as the accrued or deferred energy dividend (kWh) facilitated by thermal storage and residential renewable energy generator like Photovoltaic (PV), made possible by the temporal decoupling of the building thermal energy and power demands. In the building under consideration, this is achieved by means of the PV array, which acts as a grid-independent electricity production device capable of converting electrical energy to thermal energy via the heat pump system, which in turn is stored in the 800 l water tank. The methodology to calculate the system flexibility is based on establishing upper and lower temperature bounds for the TES system, knowledge of the TES thermophysical characteristics, the heat pump rating and the PV system rating. In the current work, the storage tank default lower and upper temperature set points were set at 35 °C and 55 °C, respectively, as outlined earlier in Table 4 (Case 3). These bounds were chosen with reference to the heat pump nominal thermal output and a system sensitivity analysis. As long as the heat pump control maintains the tank temperature T_{tk} between T_{max} and T_{min}, the TES system can be used to meet the heat demand of the building. If the temperature of the TES is close to the T_{max}, as illustrated in Fig. 8 between 0200 h and 0700 h, the shifting potential is close

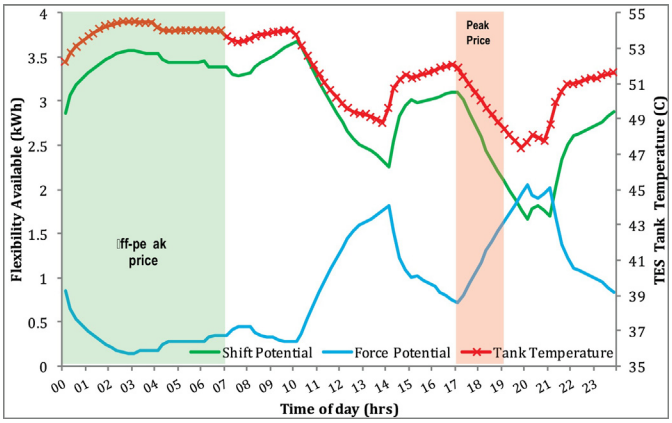

Fig. 8. Yearly average flexibility potential for time of use price signal.

to its maximum. During such period, the building can be heated by discharge of the TES, without active use of the heat pump, until T_{tk} reaches T_{min}, where the equivalent amount of electricity that is deferred or shifted (kWh) is given by Eq. (4) as follows:

$$S(t) = PV(t+dt) + \int_{t}^{t+1} \frac{Cpw \times M \times (T_{tk}(t) - T_{min})}{3.6 \times 10^6 \times COP_{hp}} dt \quad (4)$$

$S(t)$ is the sum of the PV power production plus any deferrable heat pump power consumption, which is provided by the TES system, where the PV output for the next time period is given by $PV(t+dt)$ and the TES potential is estimated with reference to the lower tank set point. This value represents the upper limit of the deferred dwelling space heating power demand plus any on-site PV electricity production.

The forcing potential $F(t)$ is calculated by Eq. (5) and is defined as the accruable heat pump power consumption when the heat pump thermal output is not used to meet the zone thermal demand but is instead stored by the TES system.

$$F(t) = \int_{t}^{t+1} \frac{Cpw \times M \times (T_{max} - T_{tk}(t))}{3.6 \times 10^6 \times COP_{hp}} dt \quad (5)$$

Although the zone temperature is equal or greater than the thermostatic set point, the heat pump can be forced to operate. In this case, the expected electric profile is altered by the forced operation of the heating system, which generates additional energy that is stored in the TES. The maximum amount of electricity (kWh) that can be used by the heat pump to charge fully the TES defines the flexibility potential.

Fig. 8 illustrates the system flexibility shifting and forcing potentials, as well as the average TES storage temperature, based on the average daily flexibility for the 2014 heating year. It can be observed that the forcing and shifting curves are inversely proportional, as they are calculated with reference to the TES upper and lower set-point temperatures. Further examination shows that the TES is fully charged at 55 °C, where the shift and forcing potential are maximised and minimised, respectively. During peak periods (17:00–19:00), the shifting potential decreases significantly because the heat pump is not operational and the building thermal load is met by the TES system, while the forcing potential increases. It can also be observed that between 14:00 and 15:00, the PV is often utilised thereby increasing the thermal energy stored in the TES tank. Figs. 9 and 10 shows the variation in hourly flexibility based on averaged data for the heating season. During the peak times from 17:00 to 19:00 h, the shifting flexibility (Fig. 9) can be observed to decrease significantly, which can be attributed to the scheduled non-operation of the heat pump. During this period, the heating system, in order to maintain zone comfort temperatures,

Fig. 9. Average hourly shifting flexibility $S(t)$.

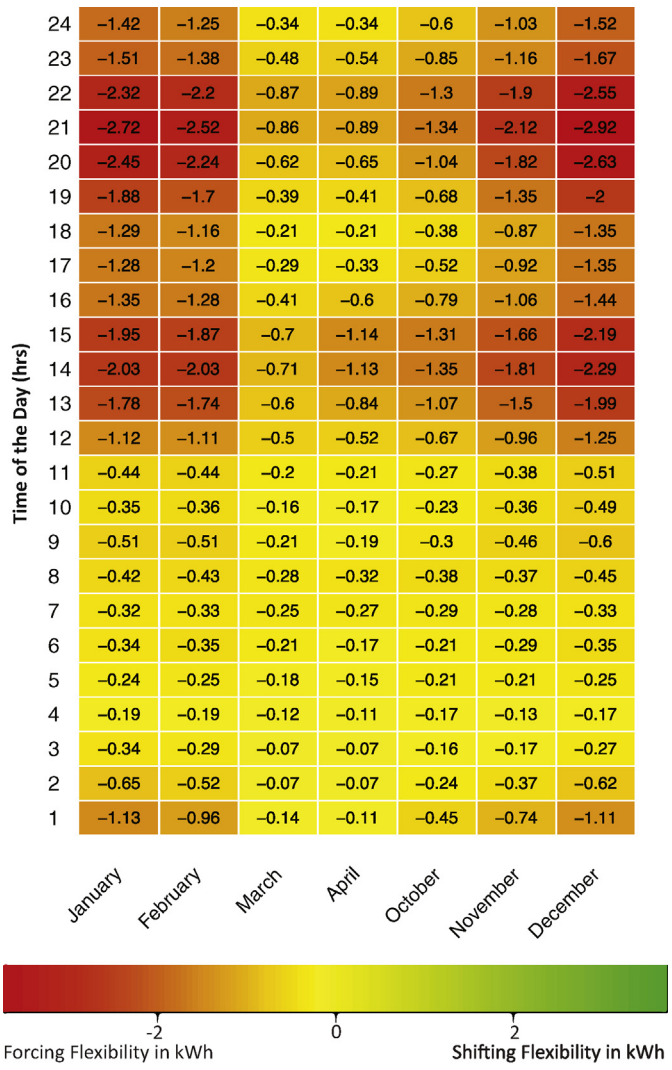

Fig. 10. Average hourly forcing flexibility $F(t)$.

extracts heat from the TES, thereby resulting in periods when the average tank temperature goes below the setpoint. Maximum shifting flexibility can be observed during the night periods, when the heating system fully charges the TES and thus exhibits a maximum shifting potential. It can also be observed that between December and February, for the period after peak time, that the forcing potential (Fig. 10) is greater that the shifting, which results from the control strategy of avoiding active use of the heat pump during peak periods, thereby resulting in the average tank temperature being closer to the lower bound.

Fig. 11 summarises the cumulative shifting and forcing flexibility for each month. Total shifting flexibility potential (is greatest for March and April, while the forcing flexibility potential is greatest for December, January and February, when the TES system often operates closest to its lowest setpoint temperature. Considering the accumulated total daily flexibility potential over the October-April period, a total shifting and forcing potential of 366 kWh and 146 kWh, respectively, exists, which if averaged on a daily basis is approximately 4.0 kWh per day or 5.5% of the heating season energy consumption.

It is noted that the two metrics reported in Eqs. (4) and (5) are an estimate of the potential flexibility available, and thus they do not give any indication of the building energy demand. Therefore, the charging and discharging rates depend on the energy demand of the building which vary based on the internal heat gains, outdoor weather conditions and temperature set points. In any case, from a grid perspective, the maximum energy that could be shifted or forced during any period, is capped by the nominal electric power consumption of the heating system. Further analysis could be performed based on the flexibility variance for different conditions to estimate the maximum duration that a demand response event could last.

4.6. Discussion

This paper proposes a rule-based algorithm that reduces the electricity expenditure of a residential building while maintaining

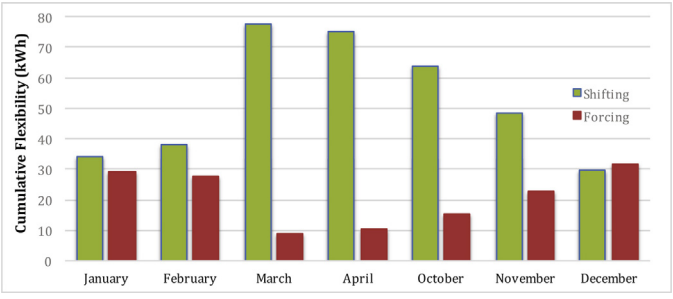

Fig. 11. Monthly cumulative flexibility potential for the heating season.

Table 6
Results summary in percentage compare to baseline.

	CO_2 emissions	Electricity consumption	Electricity cost (tariff D)	Generation cost
Case 1	−7.6%	−4.1%	−4.9%	−22.5%
Case 2	−26.4%	−13.9%	−16.2%	−44.3%
Case 3	−27.0%	−15.9%	−16.5%	−45.3%

the thermal comfort for the occupants. The control system is designed to optimise energy consumption using the heating system, the building thermal features and to provide flexibility to reduce peak load or respond to DR events based on a time use tariff scheme. The algorithm was tested using three test cases against a baseline. Referring to Table 6 and with reference to the baseline case, Case 1 illustrates the potential benefits arising from the DR measures alone, which are accrued through the PV and TES systems only. The results show a 22.5% reduction in generation cost, a 4.1% reduction in energy consumption, a 4.9% reduction in electricity end-use costs and a 7.6% reduction in carbon emissions all relative to the baseline. Case 2 shows the increased operational efficiency compared to Case 1 resulting from better setpoint control of the bedroom zones. These include an additional electricity cost reduction of up to 11.3% (Tariff A), as well as a decrease of 18.8% in associated CO_2 emissions and a reduction in the electricity consumption of 9.8%. Case 3 shows a limited reduction of emission (0.6%) and a decreased electricity demand (2%) due to the lower PV output threshold. The control system, which is based on the presented rule-based algorithm, is capable of being easily implemented and installed in buildings with different characteristics, by adapting the parameters outlined in Table 4.

However, in the case of high penetration percentage in the residential building stock, the algorithm could pose some challenges to grid operators. The first problem involves the simultaneous switching ON or OFF of the heating systems after and before a TOU peak price signal, which could result in a significant peak clipping and shifting. A solution to smooth any peak clipping and the associated rebound effect is to wait a random time interval before switching on the heating system after the DR signal. Other challenges can be associated with the tuning of the parameters for different building categories and to adapt the settings for multiple or dynamic peak windows.

Compared to other work, it should be noted that the algorithm proposed does not require sophisticated hardware or different training periods to be utilised for various building type and it was implemented and tested in a calibrated EnergyPlus simulation environment. Furthermore, the overall end-use cost reduction of the rule-based algorithm is 16.5%, lower than more complex algorithms. Kolotsa et al. [21] estimated an average electricity bill reduction of 23% for the heating system while Mohsenian et al. [18] indicate an overall 25% reduction. The unique feature of the associated control system is the flexibility metric that is independent of the building where it is installed. Flexibility is a function of the charge status of TES, the nominal power of the heating system and local renewable energy production. At each time step, the algorithm outputs flexibility in terms of forcing and shifting potential. This metric can be dynamically used by DR aggregators to calculate aggregate flexibility potential at each time step and design a signal to trigger the DR event.

5. Conclusion

In the current study, a rule-based demand response algorithm is applied to a residential building which resulted in energy and carbon emission reduction as well as monetary savings, while maintaining thermal comfort. The algorithm was developed to minimise the electricity expenditure under TOU tariff, enhancing the control of zone temperature. The study shows the results of two different versions of the control algorithm; the first version implements DR measures and on-site renewable and TES control while in the second version the zone thermal control features have been enabled. The simulation results of the first control version show a reduction of generation cost (−22.5%), electricity end-use cost (−4.9%) and carbon emission (−7.6%). In the case of zone thermal control features enabled, a reduction of up to 15.9% in annual electricity consumption, compared to a baseline reference system, was achieved. Furthermore, annual monetary savings of up to 20% (Tariff D) in end-use electricity costs, as well as a decrease of 27% in associated CO_2 emissions were also evident. In the context of the dwelling under consideration, it was also shown that electricity utilities can reduce the cost of generation by up to 45.3%. The heating system can provide 366 kWh in load shifting flexibility and 146 kWh in forcing flexibility, which together represents approximately 5.5% of the annual heating load. At a more general level, given the increasing likelihood of the adoption of TOU tariffs in many European countries, the use of advanced demand response control, such as rule-based control, coupled with thermal storage in all-electric residential buildings can positively contribute to the power system flexibility as well as reducing the electricity costs and carbon footprint of EU building stock. Further research on algorithms, which can adapt on the basis of end-user behaviour, occupant preferences could further enhance the capabilities of the described approach.

Acronyms

APE	average percentage error
CPP	critical peak price
DHW	domestic hot water
DR	demand response
DSM	demand side management
EMS	energy management system
EV	electric car
HRV	heat recovery ventilation
PV	photovoltaic
RTP	real time price
SMP	system marginal price
TES	thermal energy storage
TOU	time of use tariff
TSO	transmission system operator
COP	coefficient of performance
CHP	combine heat and power

Acknowledgements

This work was conducted in the Electricity Research Centre, University College Dublin, Ireland, which is supported by the Commission for Energy Regulation, Bord Gis Energy, Bord na Mna Energy, Cylon Controls, EirGrid, Electric Ireland, Energia, EPRI, ESB International, ESB Networks, Gaelectric, Intel, SSE Renewables, and UTRC. This publication has emanated from research conducted with the financial support of PRLTI [R12681]. The authors would like to thank the building owner for his essential support.

References

[1] DCENR, Department of Communication Energy and Natural Resources – Strategy for Renewable Energy: 2012–2020, 2012 http://www.socialjustice.

ie/sites/default/files/attach/policy-issue-article/3156/2012-05-29-strategyforrenewableenergy2012-20201.pdf.
[2] L. Pérez-Lombard, J. Ortiz, C. Pout, A review on buildings energy consumption information, Energy Build. 40 (3) (2008) 394–398.
[3] P.B. Eriksen, T. Ackermann, H. Abildgaard, P. Smith, W. Winter, J.R. García, System operation with high wind penetration, IEEE Power Energy Mag. 3 (6) (2005) 65–74.
[4] V. Hamidi, F. Li, F. Robinson, Demand response in the UK's domestic sector, Electr. Power Syst. Res. 79 (12) (2009) 1722–1726.
[5] H.C. Gils, Assessment of the theoretical demand response potential in Europe, Energy 67 (2014) 1–18.
[6] M.A. Piette, D. Watson, N. Motegi, S. Kiliccote, E. Linkugel, Automated Demand Response Strategies and Commissioning Commercial Building Controls, Lawrence Berkeley National Laboratory, 2006.
[7] S. Nolan, M. OMalley, Challenges and barriers to demand response deployment and evaluation, Appl. Energy 152 (2015) 1–10, http://dx.doi.org/10.1016/j.apenergy.2015.04.083.
[8] L. Dale, D. Klaar, L. Fischer, J. Rodriguez, F. Vermeulen, W. Winter, European wind integration study (EWIS) for a successful integration of wind power into European transmission system, in: 2008 IEEE Power and Energy Society General Meeting – Conversion and Delivery of Electrical Energy in the 21st Century, 2008, pp. 1–2, http://dx.doi.org/10.1109/PES.2008.4596648.
[9] M.R. Alam, M.B.I. Reaz, M.A.M. Ali, A review of smart homes: past, present, and future, IEEE Trans. Syst. Man Cybern. C: Appl. Rev. 42 (6) (2012) 1190–1203.
[10] T. Sweetnam, C. Spataru, M. Barrett, Exploring Price as a Demand Response Control Signal, 2014.
[11] M.H. Albadi, E. El-Saadany, A summary of demand response in electricity markets, Electr. Power Syst. Res. 78 (11) (2008) 1989–1996.
[12] E. Veldman, M. Gibescu, H. Slootweg, W. Kling, Impact of electrification of residential heating on loading of distribution networks, in: 2011 IEEE Trondheim PowerTech, 2011, pp. 1–7.
[13] IEA, International energy agency – energy-efficient buildings: Heating and cooling equipment, Tech. rep., IEA, 2011 https://www.iea.org/publications/freepublications/publication/buildings_roadmap.pdf.
[14] J. Hong, N.J. Kelly, I. Richardson, M. Thomson, Assessing heat pumps as flexible load, Proc. Inst. Mech. Eng. A: J. Power Energy 227 (1) (2013) 30–42.
[15] F. Tahersima, J. Stoustrup, S.A. Meybodi, H. Rasmussen, Contribution of domestic heating systems to smart grid control, in: 2011 50th IEEE Conference on Decision and Control and European Control Conference (CDC-ECC), IEEE, 2011, pp. 3677–3681.
[16] J.C. Fuller, K.P. Schneider, D. Chassin, Analysis of residential demand response and double-auction markets, in: 2011 IEEE Power and Energy Society General Meeting, IEEE, 2011, pp. 1–7.
[17] T. Nuytten, B. Claessens, K. Paredis, J. Van Bael, D. Six, Flexibility of a combined heat and power system with thermal energy storage for district heating, Appl. Energy 104 (2013) 583–591.
[18] A.-H. Mohsenian-Rad, A. Leon-Garcia, Optimal residential load control with price prediction in real-time electricity pricing environments, IEEE Trans. Smart Grid 1 (2) (2010) 120–133.
[19] Q. Hu, F. Li, Hardware design of smart home energy management system with dynamic price response, IEEE Trans. Smart Grid 4 (4) (2013) 1878–1887.
[20] D. Ren, H. Li, Y. Ji, Home energy management system for the residential load control based on the price prediction, in: 2011 IEEE Online Conference on Green Communications (GreenCom), 2011, pp. 1–6, http://dx.doi.org/10.1109/GreenCom.2011.6082525.
[21] D. Kolokotsa, K. Niachou, V. Geros, K. Kalaitzakis, G. Stavrakakis, M. Santamouris, Implementation of an integrated indoor environment and energy management system, Energy Build. 37 (1) (2005) 93–99.
[22] SEAI, Residential Energy Road Map, 2011 http://www.seai.ie/Renewables/Residential_Energy_Roadmap.pdf.
[23] CER, Commission for Energy Regulation – Demand Side Vision for 2020, 2011 http://www.cer.ie/docs/000654/cer11078.pdf.
[24] ASHRAE, Measurement of Energy and Demand Savings, ASHRAE Guideline 14-2002, 2002, pp. 17.
[25] E.C. Irish Government Publications, Building Regulations 2011, Conservation of Fuel and Energy – Dwellings, Section L, 2001.
[26] Ireland Central Statistics Office – The Roof Over Our Heads, 2011, pp. 60 http://www.cso.ie.
[27] Energy Plus – Engineering Reference Manual, Building Technologies Program, US Department of Energy (DOE), 2008 https://energyplus.net/sites/default/files/pdfs_v8.3.0/EngineeringReference.pdf.
[28] C. Ahern, P. Griffiths, M. O'Flaherty, State of the Irish housing stock–, modelling the heat losses of Ireland's existing detached rural housing stock & estimating the benefit of thermal retrofit measures on this stock, Energy Policy 55 (2013) 139–151.
[29] Handbook Fundamentals, ASHRAE American Society of Heating, Refrigerating and Air Conditioning Engineers, Atlanta, 2001–2005 (Chapters 26, 27).
[30] W.J. Smith, Can EV (electric vehicles) address Ireland's carbon emissions from transport? Energy 35 (12) (2010) 4514–4521.
[31] F. Marra, G.Y. Yang, C. Traholt, E. Larsen, C.N. Rasmussen, S. You, Demand profile study of battery electric vehicle under different charging options, in: 2012 IEEE Power and Energy Society General Meeting, IEEE, 2012, pp. 1–7.
[32] F. Pallonetto, S. Oxizidis, D. Finn, Exploring the demand response potential of a smart-grid ready house using building simulation software, in: IBPSA Building Simulation Conference, 2013.
[33] L. Lundstrom, Weather Data for Building Simulation: New Actual Weather Files for North Europe Combining Observed Weather and Modeled Solar Radiation, 2012.
[34] CER, Commission for Energy Regulation – DS3 System Services Technical Definitions, 2013 http://www.allislandproject.org/GetAttachment.aspx?id=28a87af5-6de5-42f4-8673-2dee3400e949.
[35] CER, Commission for energy regulation – smart metering cost-benefit analysis and trials findings reports, 2012 http://www.cer.ie/en/information-centre-reports-and-publications.aspxarticle=c03aebf5-8048-456c-ba8b-3a79319a818.
[36] P.G. Ellis, P.A. Torcellini, D.B. Crawley, Simulation of Energy Management Systems in EnergyPlus, National Renewable Energy Laboratory, 2008.
[37] SEMO, Single Electricity Market Operator, 2016 http://www.sem-o.com/Pages/default.aspx.
[38] J. Torriti, M.G. Hassan, M. Leach, Demand response experience in Europe: policies, programmes and implementation, Energy 35 (4) (2010) 1575–1583.